Pergamon

CEMENT AND CONCRETE RESEARCH

Cement and Concrete Research 29 (1999) 1019–1025

Aggregate-cement paste interface
Part I. Influence of aggregate geochemistry

William A. Tasong[1,*], Cyril J. Lynsdale, John C. Cripps

Centre for Cement & Concrete, Department of Civil & Structural Engineering, The University of Sheffield, Mappin Street, Sheffield, S1 3JD, UK

Received 16 January 1998; accepted 23 March 1999

Abstract

The influence of aggregate geochemical properties on the development of the microstructure and bond strength at the interfacial transition zone (ITZ) between aggregate and the hydrating cement paste was studied. The mineral phases and microstructure at the ITZs of three commonly used concrete aggregates (quartzite, basalt, and limestone) with contrasting chemical properties were analysed using scanning electron microscopy with an energy dispersive X-ray analyser and X-ray diffraction. It was observed that differences in microstructure and mineral phases exist at ITZ between the three different aggregates studied. The limestone in particular produced a porous ITZ as a result of chemical interaction.

Keywords: Reaction; Interfacial transition zone; Microstructure; Bond strength; Aggregate geochemistry

The mechanical behaviour and durability of concrete are thought to be affected by the microstructure of the ITZ, which differs in terms of morphology, composition, density, and other features, from the microstructure of the bulk cement paste [1–3].

The processes responsible for the formation of the ITZ are not well understood. It has been proposed [1–7] that the mechanisms responsible for its formation appear to be associated with the migration through the zone, which has high porosity, of the more mobile ions (Ca^{2+}, Al^{3+}, and SO_4^{2-}) during hydration of the cement paste. The high porosity results from the arrangement of the cement grains in contact with the aggregate. Due to the marked differences in porosity at the ITZ compared with the bulk cement paste, mineralogical growth is more favourable on the aggregate than in the paste [8]. The differential diffusion of ions promotes the heterogeneous nucleation and growth of CH and other hydration products in contact with the aggregate from an oversaturated solution [9].

Some investigations [10–12] have contrasted the formation of hydration products at the ITZ for lightweight aggregate with those for natural rock aggregates and have attributed these differences to the chemical state of the surface of the lightweight aggregate. Other studies have shown that the use of aggregates such as carbonate rock significantly affects the amount and orientation of CH crystals in the ITZ [13,14].

In general, the literature is mainly concerned with the role of the cementitious matrix in the development of the ITZ and only little attention is given (e.g., Farran [15]) to the role played by the aggregates. It is uncertain whether this biased emphasis on the cementitious matrix is accidental or is due to the misconception that aggregates are inert as inferred in certain literature. It has been demonstrated recently, however, that certain aggregates are capable of absorbing or supplying ions by leaching [16,17]. Thus, while some understanding of the ITZ microstructure has been developed from the viewpoint of the cementitious matrix properties, further research is needed to provide a complete understanding of the importance of aggregate chemical properties with respect to the buildup of ions at the ITZ, the subsequent nucleation of new mineral phases, and the development of microstructure in this zone.

In the present study the influence of the geochemical properties of natural rock aggregates on the nature of the ITZ was determined. Evidence that the ITZ microstructure and bond strength are influenced by the geochemistry of a natural rock aggregate is presented. The aim of this investigation, which forms part of a study into aggregate-cement paste bonding mechanisms in concrete, is to enrich our understanding of the importance of aggregate chemical prop-

* Corresponding author. Tel.: +44-1443-482155; fax: +44-1443-482169.
E-mail address: watasong@glam.ac.uk (W.A. Tasong)

[1] Present address is Centre for Research in the Built Environment, University of Glamorgan, Pontypridd, Wales CF37 1DL, UK.

0008-8846/99/$ – see front matter
PII: S0008-8846(99)00086-1

erties with respect to the nucleation and growth of new mineral phases at the ITZ and also to enable advances in the field of high performance concrete to be made.

1. Experimental procedures

1.1. Materials

Three typical concrete aggregate rocks were chosen for the study. These were selected to have contrasting chemical interaction with the cement paste. Petrographic analysis of the rocks used was carried out using X-ray diffraction (XRD) and also thin sections prepared from the rocks and analysed using optical microscopy. The petrology of the rocks was as follows.

The basalt aggregate samples were obtained from a quarry working a basaltic intrusion into the Carboniferous Limestone of Derbyshire, UK. In hand specimens, the rock was dark greenish-grey, fine-grained with a crystalline texture. The rock showed discoloration (reddish-brown to pinkish-brown) on exposed surfaces, which were visible signs that the rock has been slightly weathered. The mineralogy as determined by XRD comprised predominantly of plagioclase (albite and anorthite), potash feldspar (sanidine), and pyroxene (augite), with minor quantities of quartz, brucite, gibbsite, and kaolinite.

The limestone aggregate samples were obtained from a Carboniferous Limestone quarry in Derbyshire, UK. In hand specimens, the rock was pale grey in colour, fine-grained with a crystalline texture. It contained a few cracks, which were about 1 to 2 mm wide and were filled with recrystallised material. The mineralogy of this aggregate as determined by XRD consists of calcite and minor quantities of quartz.

The quartzite aggregate samples were collected from alluvial workings in terrace gravel/cobbles from the Trent Valley at Rampton, Nottinghamshire, UK. In hand specimens, the rock was pinkish white in colour, fine- to medium-grained with a crystalline texture. Its mineralogy as determined by XRD consists of quartz with minor quantities of microcline feldspar.

The cement used was ordinary portland cement (OPC). The chemical composition of the cement and the rocks in terms of major oxides as determined by X-ray fluorescence (XRF) are given in Table 1.

Table 1
Chemical composition of cement and aggregates obtained using XRF

	Percentage composition by mass			
Composition	OPC	Basalt	Quartzite	Limestone
SiO_2	20.79	49.62	96.23	1.35
Fe_2O_3	3.80	11.04	0.54	0.02
Al_2O_3	4.52	14.93	1.26	0.02
CaO	63.54	8.22	0.02	54.39
MgO	1.19	7.69	0.05	0.24
SO_3	2.88	0.02	0.03	0.05
Na_2O	0.42	2.72	0.10	0.10
K_2O	0.76	0.43	0.53	0.01
P_2O_5	0.12	0.16	0.02	0.01
TiO_2	0.20	1.71	0.14	0.01
MnO	0.08	0.15	0.01	0.01
LOI at 800°C	1.14	2.24	1.04	42.28
Total	99.44	98.89	99.79	98.31

1.2. Preparation of specimens

In order to study the influence of aggregate chemistry on the microstructure of the ITZ, test specimens were prepared for SEM-energy dispersive X-ray analyser (EDAX) analysis as shown schematically in Fig. 1. The aggregates were sawed up into 20 × 40 × 5 mm slices and a layer (approximately 5 mm thick) of cement paste [water/cement ratio (w/c) = 0.37] was applied between pairs of aggregate slices in a perspex mould. sawed aggregate surfaces were preferred over polished surfaces in order to allow comparison with similar surfaces used to study bond strength. The specimens were compacted on a jolting table normally used for testing flow of mortar according to BS 4551: 1980. The specimens were covered with wet cloth and polythene sheet and left in the laboratory for 24 h after which they were demoulded, wrapped up in wet cotton cloth, put in secured polythene bags, and stored in a mist room maintained at 21°C and 96% relative humidity until tested after 4 and 24 weeks. In order to analyse the microstructure of the ITZ, thin slices (approximately 10 mm wide) were sawed out of the specimen as shown in Fig. 1 using acetone-lubricated diamond saw. The composite specimen was fractured along the interface and both the cement paste side and the aggregate side were analysed using SEM-EDAX.

In order to study the influence of aggregate geochemical properties on the bond strength at the ITZ, test specimens were prepared as shown schematically in Fig. 2. The specimens were compacted and cured in the same manner as those specimens for SEM-EDAX analysis. Testing for bond strength was carried out by pulling the specimens (Fig. 2) apart using a Hounsfield tensometer (Hounsfield Test Equipment Ltd, Surrey, UK) after 1, 4, 12, 24, and 48 weeks. After testing for bond strength, the fractured surfaces were analysed for mineral phases using XRD. For each of the cement-paste aggregate combinations, a layer was abraded from the cement paste side at the ITZ and the powders were

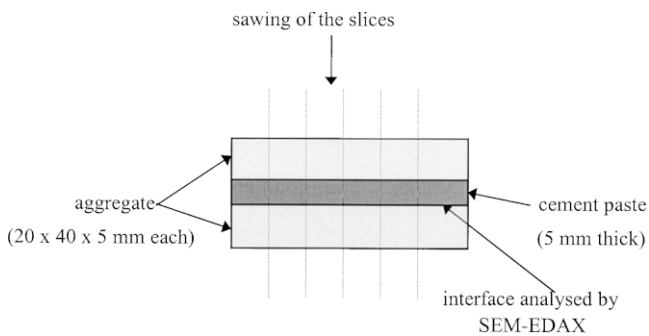

Fig. 1. Schematic representation of test specimen for SEM-EDAX analysis.

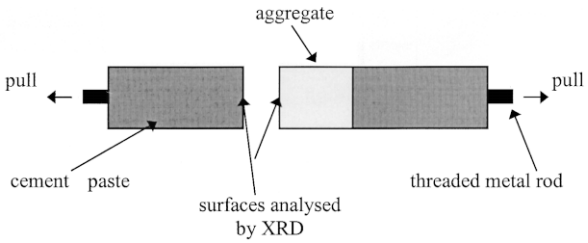

Fig. 2. Schematic representation of test specimens for XRD and ICP-AES analyses.

analysed by XRD. The thickness of the material removed ranged between 30 and 61 μm (Table 2),which falls within the range of estimated thickness of the ITZ reported in the literature [5,18–20].

2. Results and discussion

There were mineralogical and microstructural differences at the ITZ for the three different aggregates studied. These are considered in terms of the effects of the aggregate chemistry on the mineralogy, microstructure, and bond strength at the ITZ. Work on the microstructure included an investigation into the formation of high porosity in the limestone ITZ and the preferred orientation of CH crystals as well as the general morphology of this zone.

2.1. The effect of aggregate geochemistry on the microstructure and mineralogy of the ITZ

Figs. 3 to 7 show SEM micrographs of the ITZs of the three different aggregates studied. Limestone aggregate has the greatest influence on the nature and character of the microstructure at the ITZ compared with the other aggregates. The ITZ around limestone aggregate was distinctively characterised by brownish reaction stains and very high porosity (Fig. 3) compared with the basalt and quartzite ITZs.

The pores were quite large in size (0.1 to 0.2 mm in diameter) and could be seen with the naked eye at the ITZ after the aggregate-cement paste composite specimens were pulled apart. The presence of low density hydration product at the limestone/cement matrix ITZ has been reported by Roy and Jiang [21]. High magnification reveals needlelike radiating crystals in the pores (Fig. 4).

Carbon dioxide gas given off as a result of a chemical interaction between the limestone and the hydrating cement paste is considered to be the main reason for this high porosity. The release of carbon dioxide was confirmed by passing the gas through limewater, which turned milky. In this, powdered limestone (particle size range between 2 to 150 μm) was reacted with cement in the presence of water in a three-necked flask and the gas produced was forced through limewater by pressurised argon gas. When the limestone and the cement were suspended separately in water and the same procedure was performed, no carbon dioxide gas was produced. This degassing effect was not observed in the other rock types studied. Petrographic analysis revealed that this particular limestone contained veins that were filled with recrystallised calcite and poorly crystalline silica, presumably associated with postdepositional volcanic activity in the area. The poorly crystalline silica could possibly interact with water to create weak acidic pockets at the limestone ITZ. Chemical interaction between this acid and

Table 2
Thicknesses of the material removed from the cement paste side at the ITZ for RXD analysis

	Thickness (μm)		
Type of aggregate	1 week	4 weeks	12 weeks
Basalt	15	46	31
Limestone	52	50	43
Quartzite	55	61	30

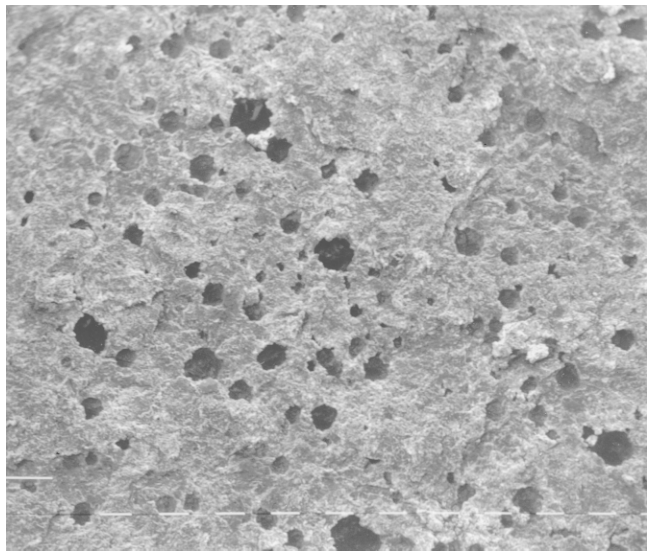

Fig. 3. Limestone ITZ, cement paste side, 4 weeks old. (Note: 1 bar = 100 μm).

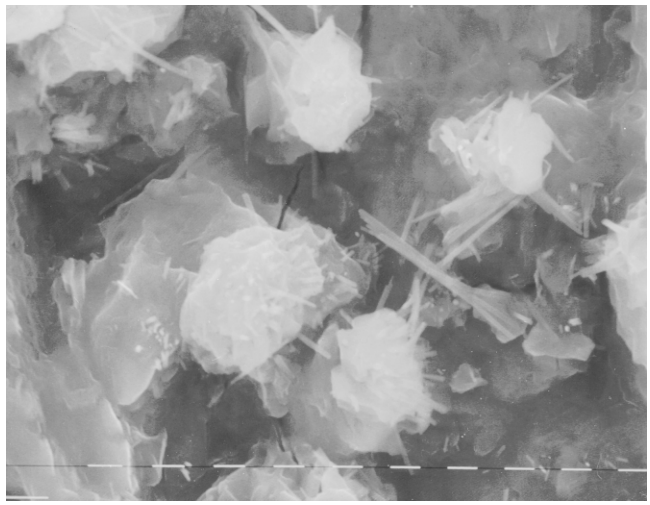

Fig. 4. High magnification of pores at the limestone ITZ, 4 weeks old. (Note: 1 bar = 10 μm).

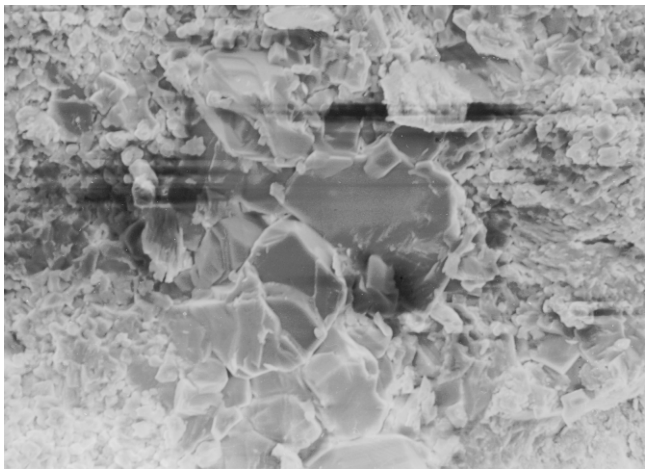

Fig. 5. CH crystals with preferred orientation at limestone ITZ (24 weeks old).

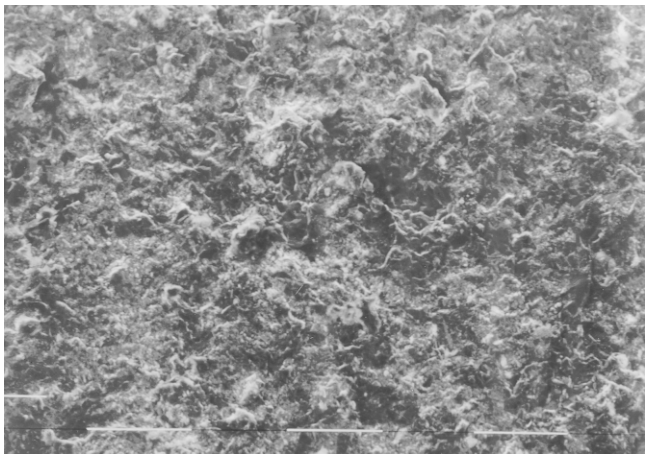

Fig. 7. Quartzite ITZ, cement paste side, 4 weeks old. (Note: 1 bar = 100 μm).

calcite, the main constituent of this limestone, is considered to be the main source of the carbon dioxide gas.

It is possible that gases released from the pores in the limestone might have contributed to the formation of the high porosity ITZ. However, the porosity of the limestone used in this investigation was quite low (3.4%). In addition, the specimens that were prepared using limestone, which had been soaked in water for over 24 h before cement paste was cast against them in a saturated but dry surface condition, produced the same high porosity ITZ.

The nonporous regions at the limestone ITZ were observed on SEM micrographs (Fig. 5) to be characterised by the presence of CH crystals with preferred orientation, particularly for the 24-week and older specimens. These were confirmed as CH crystals by performing EDAX spot analyses, which showed them to be predominantly composed of calcium. A similar observation of CH with preferred orientation has been reported for marble-cement paste ITZ [13]. In contrast, again using SEM techniques, CH crystals were not observed at the ITZ around basalt and quartzite. Cleavage surfaces at the quartzite ITZ were covered with a mesh of small ettringite crystals on the aggregate side (Fig. 6). A similar observation involving the presence of ettringite crystals either in distinct crystals or clusters, seen in direct contact with quartz aggregate surface, has been reported by Monteiro and Mehta [22]. The cement paste side did not show any microstuctural differences compared with the bulk paste (Fig. 7). Similarly, there was no noticeable difference in microstructure at the basalt ITZ compared with the bulk cement paste. Poor packing of cement particles was probably the main reason for the porosity at the ITZ around basalt and quartzite at early ages. This porosity was not observed in the 24-week or older specimens due either to pores being filled with cement hydration products or products of the pozzolanic reaction between the Si^{4+} leached out of these rocks and CH.

Fig. 6. Quartzite ITZ, aggregate side, 4 weeks old. (Note: 1 bar = 10 μm.)

According to Grandet and Ollivier [18], the ITZ is characterised by the formation of CH crystals with a preferred orientation with their c-axes normal to the aggregate surface. This degree of preferred orientation is known to decrease with distance from the ITZ until the bulk cement paste is reached where crystals are randomly orientated. Where the CH exhibits random orientation the ratio between the heights of the 2θ equals to 18.1° (001 crystal plane) and 2θ equals to 34.1° (101 crystal plane) peak heights is close to 0.74. This is the ratio obtained with a standard powdered sample of CH. According to Grandet and Ollivier the orientation index can be defined as Eq. (1):

$$\text{Orientation index} = \frac{\text{intensity}(001)}{\text{intensity}(101) \times 0.74} \quad (1)$$

Where an index of unity represents a random arrangement and an index greater than one represents increasingly more crystals orientated with their c-axes perpendicular to the ITZ.

As Fig. 8 shows, the CH orientation index at the ITZ around basalt increased sharply during the first 4 weeks, indicating increased preferred orientation. After 4 weeks it be-

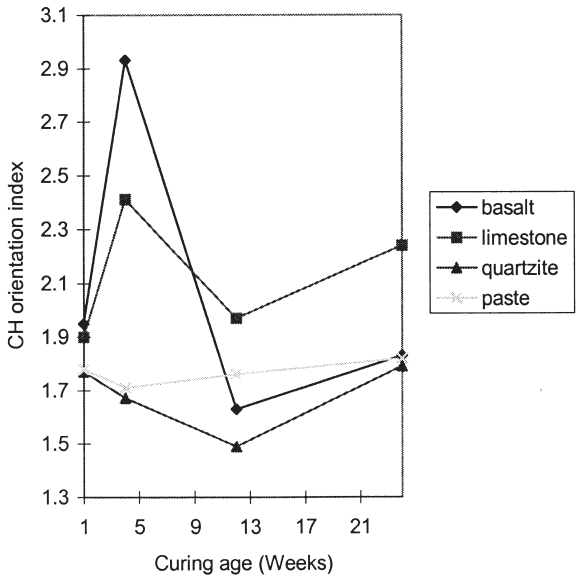

Fig. 8. The effects of rock type on the CH orientation index at the ITZ.

gan to decrease until the twelfth week after which it became similar to that of the bulk cement paste. For the limestone ITZ the CH orientation index increased gradually during the first 4 weeks after which it appeared to stay fairly constant, although still higher than that of the bulk paste. In contrast, the CH orientation index at the quartzite ITZ was more or less the same as that of the bulk cement paste at all ages studied.

The low CH orientation index at the quartzite ITZ could be due to a pozzolanic reaction between the Si^{4+}, leached out of this rock as previously observed [16,17], and the CH or the hydroxyl ion to produce calcium silicate (CSH), which is known to enhance the density of the ITZ and increase bond strength [23,24]. On the other hand, the decrease in the CH orientation index at the basalt ITZ could be due to the following two reasons: First, a pozzolanic reaction may have occurred between the Si^{4+}, leached out of this rock and the CH in a similar manner as for quartzite. Basalt was previously observed [16,17] to produce a hydrating surface layer when in contact with the cement solution and this layer released Si^{4+} into the cement solution and absorbed the hydroxyl ion. Second, a chemical interaction between CH and feldspars or clay minerals in this rock might have occurred. CH is known to react with feldspars to produce tetracalcium aluminate hydrate [25].

The fact that the drop in the CH orientation index at the basalt ITZ occurs after 4 weeks may suggest that these reactions only start some 4 weeks after hydration. Alternatively, it could be due to the cement hydration processes, which could have slowed down after 4 weeks, thereby resulting in a reduced supply of CH while the chemical reactions between the aggregate and the CH were still taking place.

In contrast to basalt and quartzite, the CH orientation index at the limestone ITZ was higher than that of the bulk paste at all ages studied. Limestone was observed previously [16,17] to release Ca^{2+} into the cement solution while having no effect on the concentration of the hydroxyl ion, which may have resulted in a more saturated pore fluid with respect to Ca^{2+} and OH^{-} at the ITZ and the subsequent growth of CH with preferred orientation from this oversaturated solution.

As Fig. 9 shows, there were differences in mineral phases formed at the ITZ between the limestone and the other rock types studied. However, there was no noticeable difference in mineral phases between the bulk cement paste and the cement paste at the ITZ around basalt and quartzite. In contrast to the ITZ around basalt and quartzite, the limestone ITZ contained carboaluminate and amorphous phases, some of which might not have been detected by XRD while others were detected by XRD but were not identified using standard XRD 2θ tables for minerals [26] and were denoted here as the Tascarbo phases. Carbonate rocks are known [18] to react with hydrating cement paste to produce carboaluminate.

2.2. Effects of aggregate geochemistry on aggregate-cement paste bond strength

Although the mechanism of bonding by chemical reaction between the aggregate and the cement matrix has been suggested in the existing literature [13,23], little or no direct evidence has been provided to support this claim. In most of these investigations, no aggregate-cement chemical interactions were investigated. In addition, the geochemical properties of the rock used as aggregate are often inadequately described or known.

The results shown in Fig. 10 reveal significant differences in the way tensile bond strength varied with curing age between the three different aggregates studied. It should be noted that these results represent the average of eight measurements with a coefficient of variation of less than 5%. Differences in their chemical properties and chemical interaction with the cement paste are considered to be the main reason for this effect. As previously observed [24], there were only minor differences in the measured characteristics of the sawed surfaces between the three rock types investigated, implying that the difference in measured bond strength are not solely due to differences in surface characteristics.

Three different modes of bond failure in direct tension tests were observed due to differences in mineralogy and structure of the rocks used. These are: mode A, in which failure cracks pass cleanly at the ITZ; mode B, in which failure cracks ran through the ITZ at some points and continued through the paste; and finally mode C, in which failure cracks ran through the ITZ at some points and continued through the paste and the aggregate.

2.2.1. Basalt

Basalt was observed to show the type A mode of failure at all curing ages studied. At 1 week, basalt achieved a bond strength value, which was higher than that of limestone but lower than that of quartzite. Its bond strength was observed to increase sharply during the first 4 weeks, after which it stayed fairly constant until the twelfth week before drop-

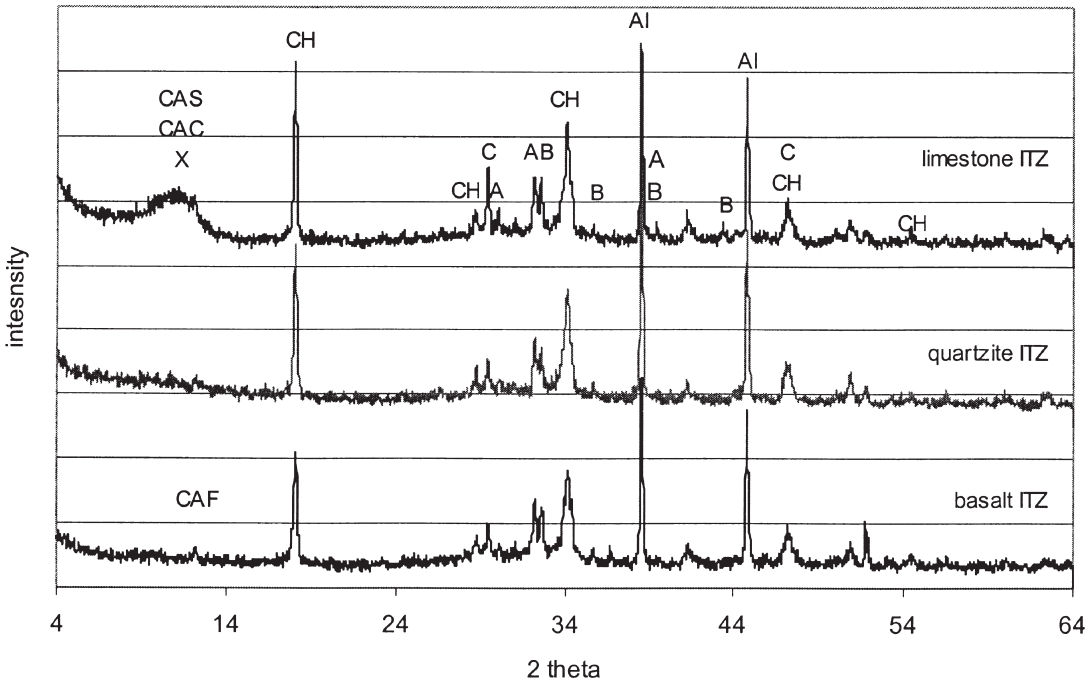

Fig. 9. X-ray powder diffraction patterns of the products formed at the ITZ at 1 week. CAS = tetracalcium aluminate monosulphate 12-hydrate; CAC = tetracalcium aluminate carbonate 12-hydrate; X = other amorphous phases that were not identified on standard 2θ table (Tascarbo phases); CH = calcium hydroxide, A = alite, B = belite, C = calcite, and CAF = ferrite; Al = aluminium (not a hydration product, but present because of the Al sample holder).

ping fairly sharply till the twenty-fourth week, after which it stayed fairly constant for the rest of the time up to the forty-eighth week. This observation contradicts the findings of Odler and Zurz [27] who reported that the cleavage strength of the basalt-cement paste composite was lower than that of limestone at all ages studied (1, 4, and 8 weeks). The early bond strength of basalt was higher than that of limestone since, first, the surface roughness of sawed basalt is slightly higher than that of limestone [24], hence the bond due to mechanical interlocking of the cement hydration product with the rough aggregate surface will be higher in basalt than in limestone. Second, and probably more significant, the porous ITZ around limestone (Fig. 3) accounts for the weak bond between this rock and the cement paste at early age.

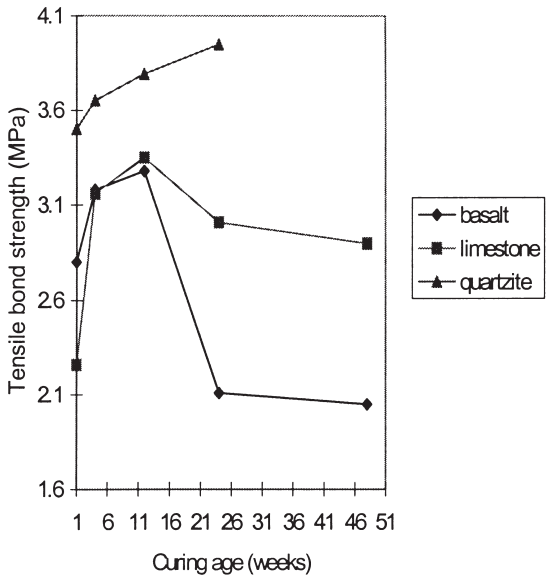

Fig. 10. Changes in aggregate-cement paste tensile bond strength with curing age.

The increase in bond strength of basalt during the first 4 weeks of continuous curing is probably due to increase in the cement hydration process that resulted in an increase in mechanical interlocking of the cement hydration products with the rough aggregate surface. The chemical break down of feldspars due to their interaction with the hydrating cement to produce clay minerals as previously observed [16], which swell on absorbing water, is considered to be the main reason for the observed decrease in bond strength of basalt after the twelfth week. Alternatively, chemical break down of feldspars and other mineral grains on the basalt surface in contact with the cement paste may reduce the surface roughness and weaken the mechanical interlocking effect between the rock surface and the hydration products, resulting in a weaker bond.

2.2.2. Limestone

Unlike basalt, limestone was observed to show three different modes of bond failure and this varied with curing age. At 1 week, limestone achieved a bond strength value lower than that of basalt or quartzite and showed a type A mode of failure. Its bond strength increased sharply during the first 4 weeks at the end of which it achieved the same bond strength as basalt and showed a type A mode of failure. By the twelfth week, limestone achieved an “apparent” bond strength lower than that of quartzite and similar to basalt,

but showed a type B mode of failure. After the twelfth week, its apparent bond strength dropped gradually till the twenty-fourth week, after which it stayed fairly constant for the rest of the time. During this period, limestone achieved an apparent bond strength, which was slightly higher than that of basalt and showed type C mode of failure.

The high initial porosity at the limestone ITZ discussed above is considered to be the main reason for the weak bond achieved by this rock at the early age. However, at latter ages, some manifestations of the development of a chemical bond between the limestone aggregate and the cement paste were evident. First, unlike the basalt, the limestone-cement paste system achieved type B and C modes of failure at the later ages due to increase in bond as a result of its chemical interaction with the cement paste. Second, the limestone ITZ was characterised by the presence of heavy brown colour reaction stains. This stronger bond strength was achieved at the later ages even with the high porosity limestone ITZ. The chemical interaction between this rock and the cement paste to produce carboaluminates as discussed above, which are know to increase bond strength [13,18], is considered to be the main reason for this increase in bond strength with increasing curing age. Although the bond strength remained high after the twelfth week, the weak mechanical strength of both limestone and the cement paste became the strength-limiting factor resulting in the weak apparent bond achieved, hence type C mode of failure occurred. The low mechanical strength of the limestone was due to the presence of large crystals of calcite in the limestone, which have low bond and tensile strength on their cleavage surfaces.

2.2.3. Quartzite

Quartzite was observed to be superior to basalt and limestone in terms of the measured bond strength. It achieved higher apparent bond strength values than either the basalt or limestone at all curing ages studied. It showed type A modes of failure at 1 week after which it showed a type B mode of failure throughout. A pozzolanic reaction between the Si^{4+} leached out of this rock as discussed above, and the hydrating cement paste that is known [23] to enhance the density of the ITZ and increase bond strength is considered to be the main reason for the high apparent bond strength achieved. Unlike limestone, quartzite had a stronger mechanical strength [16,24] and the cement paste was observed to be the strength limiting factor, and hence the type B mode of failure shown.

3. Conclusions

The results show that unlike basalt and quartzite, the limestone used in this study reacted with the cement paste to produce a very porous ITZ due to the release of CO_2 gas. This porous ITZ was characterised by brown stains and also contained amorphous and carboaluminate phases.

The CH at the limestone ITZ showed some degree of preferred orientation in which the c-axis was perpendicular to the aggregate surface. A similar effect was not detected at the quartzite ITZ, whereas with the basalt ITZ, preferred orientation was recorded during the first 4 weeks after which the CH became randomly orientated.

Chemical interaction between some rocks and cement paste may lead to a reduction rather than an increase in bond strength. In particular, limestone reacted with cement paste to produces a very porous ITZ, which resulted in a reduction in bond strength an early age. However, at later ages, filling of this porosity with later reaction products resulted in an increase in bond strength.

Chemical reaction between basalt and the cement paste resulted in a reduction of bond strength after 12 weeks of continuous curing.

Acknowledgments

Financial support by the Centre for Cement & Concrete (CCC) at the University of Sheffield where this work was carried out is gratefully acknowledged. The authors would also like to thank the technical staff of the Centre and the Department of Earth Sciences at the University of Sheffield for their technical support during the experimental work.

References

[1] L. Struble, J. Skalny, S. Mindess, Cem Concr Res 10 (1980) 277.
[2] J.C. Maso, in: 7th Int. Cong. Chem. Cem., Vol. I, Paris, 1980, p. VII-1/3.
[3] S. Mindess, I. Odler, J. Skalny, in: 8th Int. Cong. Chem. Cem., Vol. I, Finep, Rio de Janeiro, Brazil, 1986, p. 151.
[4] D.B. Barnes, S. Diamond, W.L. Dolch, Cem Concr Res 8 (1978) 233.
[5] P.J.M. Monteiro, J.C. Maso, J.P. Ollivier, Cem Concr Res 15 (1985) 953.
[6] D. Breton, A. Carles-Gibergues, J. Grandet, Cem Concr Res 23 (1993) 335.
[7] L. Struble, Mat Res Soc Symp Proc 114 (1988) 11.
[8] A. Carles-Giberues, F. Saucier, J. Grandet, M. Pigeon, Cem Concr Res 23 (1993) 43.
[9] C.Z. Yuan, W.J. Guo, Cem Concr Res 17 (1987) 544.
[10] W. Yuji, Mat Res Soc Symp Proc 114 (1988) 49.
[11] Z. Min-Hong, O.E. Gjorv, Cem Concr Res 20 (1990) 610.
[12] L. Stevula, J. Madej, J. Kozankova, J. Madejova, Cem Concr Res 24 (1994) 413.
[13] P.J.M. Monteiro, P.K. Mehta, Cem Concr Res 16 (1986) 127.
[14] M. Siato, M. Kawamura, Interfaces in Cementitious Composites, in: Proc. of the RILEM Intl. Conf. Vol. 18, 1993, p. 33.
[15] J. Farran, Revue des Materiaux de Construction 490–491 (July–August 1956) 155–172; and 492 (September 1956) 191–209.
[16] W.A. Tasong, Ph.D. Thesis, Department of Civil & Structural Engineering, University of Sheffield; Sheffield, UK, 1997.
[17] W.A. Tasong, J.C. Cripps, C.J. Lynsdale, Cem Concr Res 28 (1998) 1037.
[18] J. Grandet, J.P. Ollivier, Cem Concr Res 10 (1980) 759.
[19] J.A. Larbi, J.M. Bijen, Cem Concr Res 20 (1990) 461.
[20] K.L. Scrivener, E.M. Gartner, Mat Res Soc Symp Proc 114 (1988) 77.
[21] D.M. Roy, W. Jiang, Mat Res Soc Symp Proc 370 (1995) 309.
[22] P.J.M Monteiro, P.K. Mehta, Cem Concr Res 16 (1986) 111.
[23] K.M. Alexander, J. Wardlaw, D.J. Gilbert, The structure of concrete, in: Proc. of Int. Conf., London, 1965, p. 59.
[24] W.A. Tasong, C.J. Lynsdale, J.C. Cripps, Cem Concr Res 28 (1998) 1453.
[25] J.H.P. Van Aardt, Visser, Cem Concr Res 7 (1977) 643.
[26] H.F.W. Taylor, The Chemistry of Cement, 2d ed., Academic Press, London, 1964.
[27] I. Odler, A. Zurz, Mat Res Soc Symp Proc 114 (1988) 21.